0273-2289/91/3102—0145$02.80

Electrochemical Studies on Tetrathiafulvalene-Tetracyanoquinodimethane Modified Acetylcholine/Choline Sensor

P. C. PANDEY,*,[1] C. TRAN-MINH, AND F. LANTREIBECQ

Laboratoire de Biotechnologie Ecole des Mines 42023 Saint-Etienne-Cedex, France; and [1]Permanent address: Department of Chemistry, Banaras Hindu University, Varanasi-221005, India

Received October 29, 1990; Accepted April 22, 1991

ABSTRACT

A sensor for acetylcholine/choline is described using a tetrathiafulvalene-tetracyanoquinodimethane (TTF-TCNQ) electrode modified with acetylcholine esterase (AChE) and choline oxidase (ChO) enzymes. DC cyclic voltammetry and impedance measurements of the enzyme-modified TTF-TCNQ electrode that indicate the regeneration of choline oxidase at the electrode surface are reported. Effective electrochemical rate constants for the present enzyme electrode are calculated using the expressions derived by Albery et al. (*1*), which show the enzyme kinetics as the rate-limiting step. The values of the effective electrochemical rate constants are close to those reported by Hale and Wightman (*2*). The application of the sensor is described for the determination of fluorode ion and nicotine based on the reversible inhibition of AChE activity. The range of detection of fluoride ion and nicotine is found to be 5×10^{-6} to 5×10^{-4}M.

Index Entries: Enzyme electrode; enzyme inhibition; frequency-response analysis; bioelectronics, neurotransmitters.

*Author to whom all correspondence and reprint requests should be addressed.

INTRODUCTION

Analysis of neurotransmitters has recently gained considerable attention (*2–4*). Potentiometric determination of acetylcholine has been described (*5,6*), but the sensitivity is inadequate for clinical purposes. Amperometric determination of choline has been described using choline oxidase (ChO) immobilized onto an oxygen electrode (*7,8*) and a chemically modified platinum electrode (*9*) as a working electrode. Simultaneous electrochemical determination of acetylcholine and choline has been described by liquid chromatography (*10*) and using immobilized AChE and ChO on nylon net (*11*). There is still need of a suitable sensor for the sensitive and selective determination of the neurotransmitters. During this decade, chemical modification of the electrode surface has attracted considerable interest for the construction of amperometric probes (*12–15*). Chemical modification of the electrode surface is achieved by the treatment of the naked metal surface using mediators and conducting polymer as electrode materials. The use of tetrathiafulvalene-tetracyanoquinodimethane (TTF-TCNQ) conducting polymer as an electrode material (*16*) is of considerable interest for the chemical modification of the electrode surface (*12–15*) because of its low background current. This conducting polymer has been used as an electrode material for the direct oxidation of ChO at the electrode surface (*2*).

In an amperometric enzyme electrode the Faradic process occurs by the direct electron exchange either from one of the enzymatic reaction products or directly from the redox center (e.g., FAD/$FADH_2$) of the enzyme. The latter normally does not occur at the conventional metal electrode surfaces because the distance between the redox center and the electrode surface exceeds the distance across which electrons are transferred at a measurable rate (*17*). Hence electrical communication between the redox center of the enzyme and the naked electrode surface requires the presence of electron-transfer relays. The use of these relays suggests two distinct means of electron exchange: (1) a mediated mechanism, which requires the presence of electron carriers reacting with the enzyme redox center and then regenerated electrochemically on the electrode and (2) a mediator-free mechanism, which involves electron exchange in absence of kinetically mobile mediators at the equilibrium potential of the substrate. Recent experimental results on conducting organic-metal electrodes suggest the dependence of the electron exchange rate on the protein nature, the electrode materials, and the state of the electrode/electrolyte interface. Kulys et al. (*19,20*) claim the mediator-free mechanism for the electron exchange from the redox center of enzyme and organic-metal electrode surface in cases of relatively low-mol-wt protein electron carrier (e.g., cytochrome b_2 and hemin), and mediated mechanism (*21*) of electron exchange in case of relatively high molecular weight enzyme, the active center of which lies deeply buried in a polypeptide structure, supported by the fact that substrate oxidation proceeds at the potentials cor-

responding to the mediator's redox conversion potential, which is formed in the layer near the electrode surface during the slight dissolution of organic metal. Reports are also available showing the extremely efficient oxidizing behavior of the components of the organic metals TCNQ (*21,22*) and TTF (*23,24*) for the reduced enzyme. These observations suggest a mediated mechanism of electron exchange between the redox center of the enzyme/protein and the organic-metal electrode. However, Albery et al. (*12*) disagree with the mediated mechanism and suggest the direct route of electron exchange from the enzymelike glucose oxidase to the organic-metal surface, citing the experimental data on the organic-metal dissolution products using the rotating ring-disk electrode, as they have not been able to detect the same, which is required for homogeneous mediation, suggested by Cenas and Kulys (*25*). Recently Albery et al (*26*) suggested that the reaction of the enzyme on the conducting organic-metal electrode proceeds through heterogeneous redox catalysis instead of direct electron transfer as proposed earlier (*12*) based on the data on reaction order with respect to enzyme, which is half, rather than unity, for direct electron-transfer. Hill et al. (*27*) have also demonstrated the application of the active layer at the interface, which fascilitates the electron transfer of soluble or weakly adsorbed enzyme through catalysis. These experimental and theoretical reports indicate three possible mechanisms for electron transfer from the redox center of the enzyme/protein to the organic-metal electrode surface: (1) homogeneous mediation, (2) direct transfer, and (3) heterogeneous redox catalysis. The present paper gives deeper insight into the mechanism of electron transfer based on these three mechanisms and the distance between the redox center and the electrode surface at which the electrons are transferred at a measurable rate. We report an AChE/ChO-modified tetrathiafulvalene-tetracyanoquinodimethane electrode for the simultaneous analysis of acetylcholine/choline. The electrochemical studies (dc cyclic voltammetry and frequency-response analysis) of the enzyme electrode are reported. The effective electrochemical rate constants for the enzyme electrode have been calculated using the expressions derived by Albery et al. (*1,28*), which show the enzyme kinetics as the rate-limiting step. The present sensor has been exploited for the determination of AChE activity, since the activity of acetylcholine esterase is inhibited in presence of certain toxics (*6,29,30*), which in turn affect the oxidation of ChO at the electrode surface.

EXPERIMENTAL

Materials

Purified AChE (EC 3.1.1.7), ChO (1.1.3.17), acetylcholine chloride, choline, and nicotine were obtained from Sigma. TCNQ, TTF, and PVC powder were obtained from Aldrich. All other chemicals were of analytical grade.

Preparation of TTF-TCNQ Electrode

The TTF-TCNQ salt was prepared according to the procedure described by Jaeger and Bard (*16*) followed by five washings in cold acetonitrile and diethyl ether alternately. The electrodes were made by placing a platinum disk (diameter 4 mm) in a Teflon™ holder having a recessed depth of 1.2 mm. The back of the platinum disk was connected to a copper wire using silver-loaded epoxy resin (Elecolite, 336 A + B). The contact resistance was < 0.2 Ohm. The platinum disk was shielded using nonconductive epoxy resin (Ciba-Geigy, HY 956 and ZY 103). This electrode was filled to a 1-mm depth with a slurry of TTF-TCNQ and PVC (13/1) in anhydrous tetrahydrofuran. The electrode was cured for 24 h at room temperature in the dark. The resistance of the TTF-TCNQ electrode was $< 100\ \Omega$. The enzyme electrode was made by soaking the TTF-TCNQ electrode in an aqueous solution of AChE/ChO for several hours.

Electrochemical Measurements

DC cyclic voltammetry, frequency-response analysis, and amperometric measurements were performed with a Tacussel-type PRT 20-2X potentiostat, Solartron Schlumberger (Farnborough, Hants) 1286 electrochemical interface, 1255 HF frequency-response analyzer and a Hewlett Packard 85 microcomputer. A Hewlett Packard plotter (model no. 7470A) was used to plot the data. The experiments were performed in a one-compartment water jacket cell with a working vol of 10 mL, using three electrodes. The temperature was controlled by an ultrathermostat (K5 COLORA messtechnik, Gmbh LORCH/WURTT) and all experiments were performed at 30°C. The reference and counter electrodes were a saturated-calomel electrode (SCE) and a platinum-wire electrode, respectively. The electrodes were secured in position in the thermostatic cell, and all the experiments were performed under argon.

Amperometric measurements of the acetylcholine/choline was performed at constant potential of 0.225 V vs SCE in 0.5*M* phosphate buffer (pH 7.5). The background current was allowed to decay to a steady-state and varying concentrations of acetylcholine/choline were injected into the reaction cell. After brief stirring the current in quiescent solution was recorded.

Determination of Fluoride Ion and Nicotine

For the determination of fluoride ion and nicotine, first the steady-state reponse was established by adding an appropriate concentration of acetylcholine. After the establishment of the steady-state, varying concentrations of fluoride ion and nicotine were injected into the reaction cell and the new steady-state was recorded. From the difference of two steady-states, the percentage of AChE inhibition was calculated at the different concentrations of the inhibitors.

RESULTS AND DISCUSSION

There has been no controversy regarding the direct electron exchange from relatively low-mol-wt electron carriers (e.g., cytochrome-c, cytochrome-c_3, ferredoxin, flavodoxin, and some other proteins) to the surface of organic-metal electrodes. However, the mechanism of electron transfer from relatively high-mol-wt enzymes whose active centers lie deeply buried in a polypeptide structure is controversial regarding whether the enzyme is oxidized by direct electron transfer or whether there is a mediated electron transfer. Evidence for mediated electron transfer includes the following observations:

1. Dependence of anodic current on the electrode potential;
2. Potential value of substrate oxidation that proceeds at the mediators' (components of organic metal) redox conversion potentials;
3. Formation of mediator in the layer near the electrode surface during the slight dissolution of organic metal; and
4. Applications of TCNQ and TTF^+ as efficient mediators for the oxidation of the reduced form of enzymes.

These observations suggest a mediated mechanism of electron transfer, rather than direct electron transfer. However, other experimental observations reported by Albery et al. (*26*) show the dependence of anodic current on the square root of enzyme concentration. This observation suggests that electron transport takes place by heterogeneous redox catalysis, rather than by direct or mediated electron transport. Hill et al. (*27*) also support the conclusion of Albery et al. (*26*). Based on the radiolabeling experimental data they suggest that when a TTF-TCNQ electrode is soaked in the enzyme solution at least two types of adsorbed layers are formed at the interface. The first one is irreversibly adsorbed and inactive, whereas the second one is weakly or reversibly adsorbed and is responsible for heterogeneous redox catalysis. There are also reports (*16*) that surface transformation of a TTF-TCNQ electrode gives symmetrical cathodic and anodic peaks because of reduction and oxidation of $TCNQ^0$ and TTF^0, respectively. We have also found that a choline sensor can be designed using ChO in acrylamide–methacrylamide–hydrazides prepolymer immobilized onto the surface of an electrochemically transformed TTF-TCNQ electrode. The membrane film containing immobilized ChO can be attached to the surface of a TTF-TCNQ elecrtode using the procedure described earlier (*6*). Fig. 1A shows the dc cyclic voltammograms of an enzyme electrode made up using immobilized ChO within the membrane and an electrochemically transformed TTF-TCNQ electrode in the absence (a_1) and presence (a_2) of 0.3 m*M* choline in 0.5*M* phosphate buffer (pH 7.5) at scan rate of 10 mV/s. These results are similar to those reported by Hill et al. (*27*). There is an increase in anodic current and a decrease in cathodic current on the addition of choline, thereby showing regeneration of ChO.

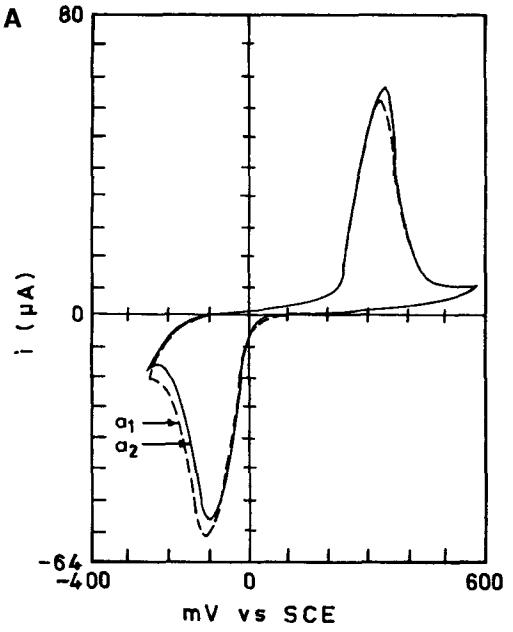

Fig. 1A. Cyclic voltammograms of electrochemically transformed TTF-TCNQ enzyme electrode in the absence (a_1) and presence (a_2) of 0.3 m*M* choline in 0.5*M* phosphate buffer, pH 7.5, at 30°C.

It appears that electron exchange from the proteins may takes place by direct electron transfer, by a mediated method, or by heterogeneous redox catalysis, depending on the method of electrode preparation and the distance between its redox center and electrode surface, since in proteins the electron transfer rates drop (*31*) by 10^4 when the distance between the electron donor and an electron acceptor is increased from 8 to 17 A. The dc cyclic voltammetry studies reported by earlier workers (*13–15*) and also in the present paper on TTF-TCNQ electrodes with and without enzyme in the absence of substrate show the same background current within the defined potential range, thereby showing that no redox reactions are occurring at the electrode surface. Further, the direct electron communication from the redox center of enzyme and naked metal electrode can be facilitated by incorporating electron-accepting/transferring relays in the enzyme without causing damaging structural change (*17*), which substantially shortened the electron-tunneling distances involved in communicating between the redox center of enzymes and the naked electrode surface. Hence direct electron transfer from the active center of enzyme to the TTF-TCNQ electrode depends on the thickness of the reaction layer, method of electrode preparation, polarity of the medium in which experiments are carried out, electrochemical pretreatment, and stability of the electrode within the desired potential range. Further, another

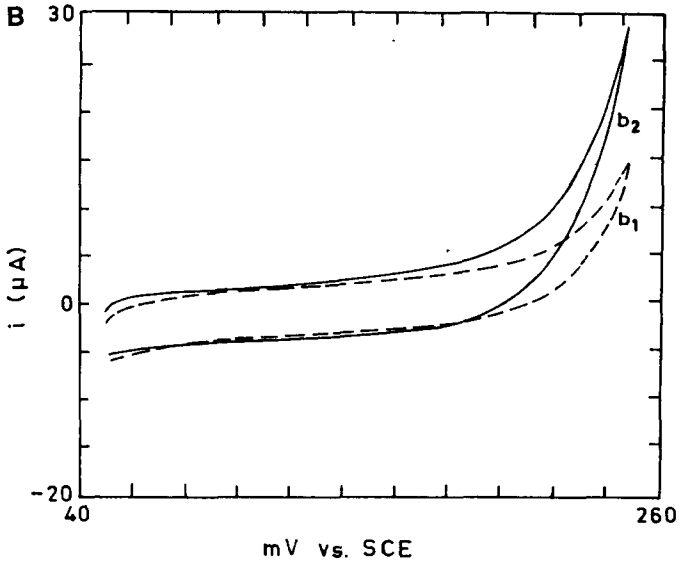

Fig. 1B. Cyclic voltammograms of AChE/ChO modified TTF-TCNQ electrode in absence (b_1) and presence (b_2) of 0.5 m*M* acetylcholine in 0.5*M* phosphate buffer, pH 7.5, at 30°C.

characteristic of the TTF-TCNQ electrode is its large surface area and roughness, which facilitate the direct electron transfer. Experimental results on dc cyclic voltammetry and impedance measurements given below support this conclusion.

Figure 1B shows the dc cyclic voltammograms of an AChE/ChO-modified TTF-TCNQ electrode in the presence and absence of 0.5 m*M* acetylcholine in 0.5*M* phosphate buffer at the scan rate of 5 mV/s. There is a increase in the anodic current on the addition of acetylcholine/choline, thereby showing regeneration of ChO at the TTF-TCNQ electrode surface.

Figures 2 and 3, respectively, show the low (1–10 kHz) and high (0.5–5 MHz) frequency responses of the enzyme-modified TTF-TCNQ electrode. The amplitude of the applied sinusoidal voltage was 225 mV. The data show the variations of impedance modulus and phase angle as a function of frequency. The low-frequency response (Fig. 2) does not give any valuable information; however, the high-frequency response (Fig. 3) shows sharp variation of impedance modulus at 3.2 MHz. On the addition of substrate there is a significant increase in the impedance modulus, thereby showing oxidation of ChO at the TTF-TCNQ surface (Fig. 3). Figure 4 shows the variation of real and imaginary parts of impedance modulus as a function of frequency; Fig. 5 shows the Nynkvist plot of thedata in Fig. 3 in the presence and absence of acetylcholine. The variations of the real and imaginary parts of the impedance modulus are quite different in the presence and absence of the substrate (Figs. 4 and 5). These results indi-

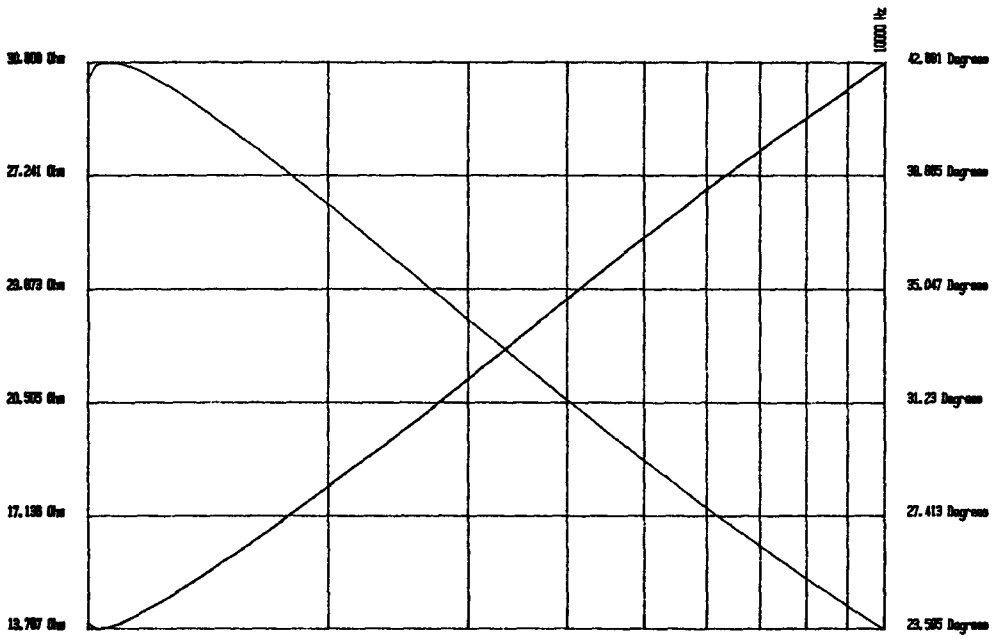

Fig. 2. Low-frequency (1–10 kHz) response of AChE/ChO modified TTF-TCNQ electrode in 0.5*M* phosphate buffer, pH 7.5, at 30°C. The data represent the variation of impedance modulus and phase angle as a function of frequency at 225 mV polarization voltage.

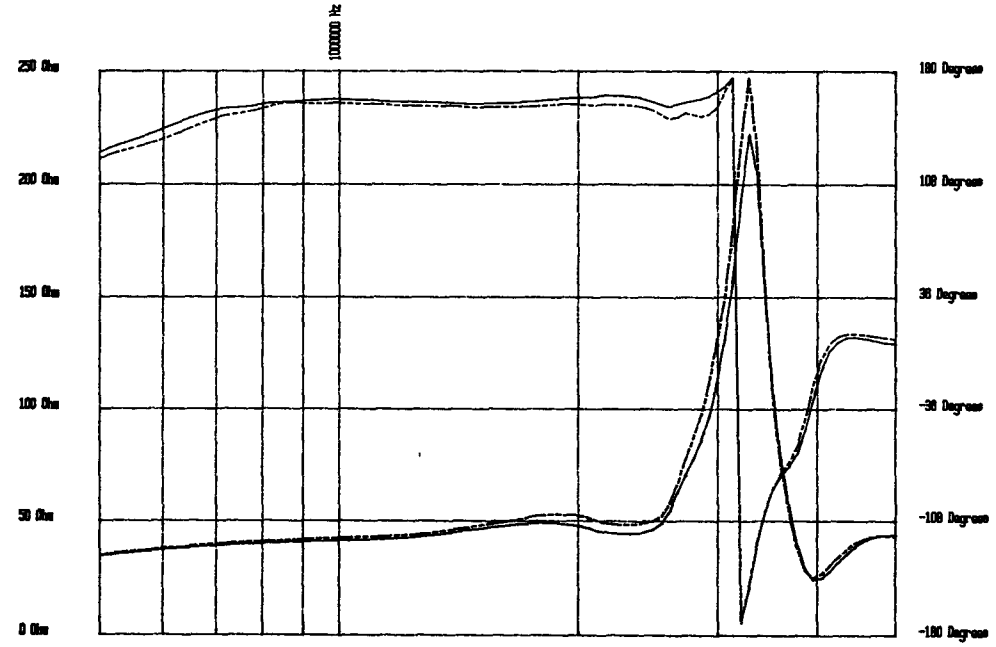

Fig. 3. High-frequency (0.5–5 MHz) response of AChE/ChO modified TTF-TCNQ electrode in the presence (dotted line) and absence (solid line) of 0.3 m*M* acetylcholine in 0.5*M* phosphate buffer, pH 7.5, at 30°C. The data represent the variation of impedance modulus and phase angle as a function of frequency at 225 mV polarization voltage.

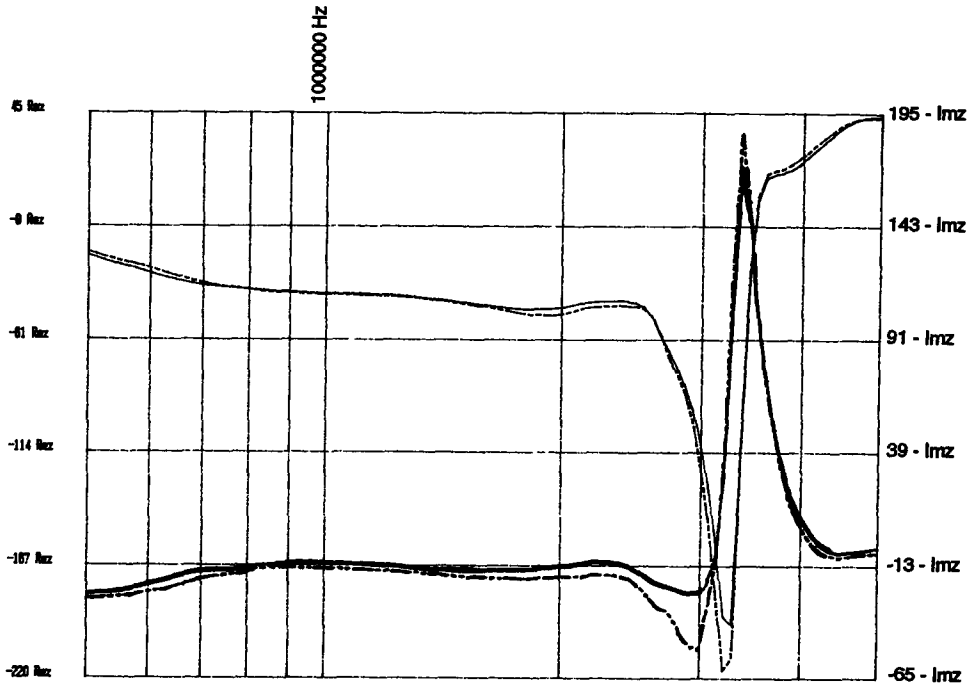

Fig. 4. Variation of real and imaginary parts of the impedance modulus as a function of frequency in the presence (dotted line) and absence (solid line) of 0.3 m*M* acetylcholine.

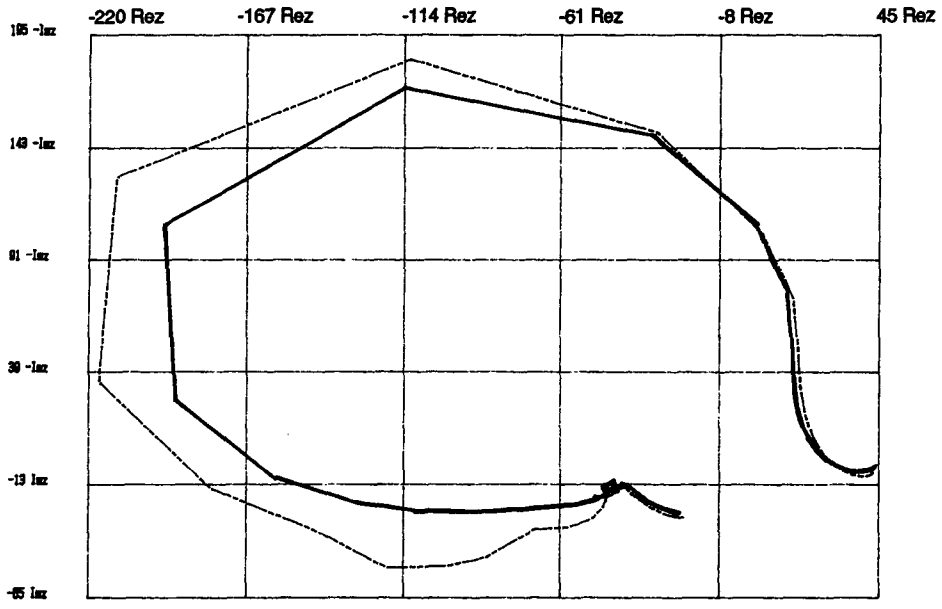

Fig. 5. Nynkvist plots of the data given in Fig. 3 in the presence (dotted line) and absence (solid line) of 0.3 m*M* acetylcholine.

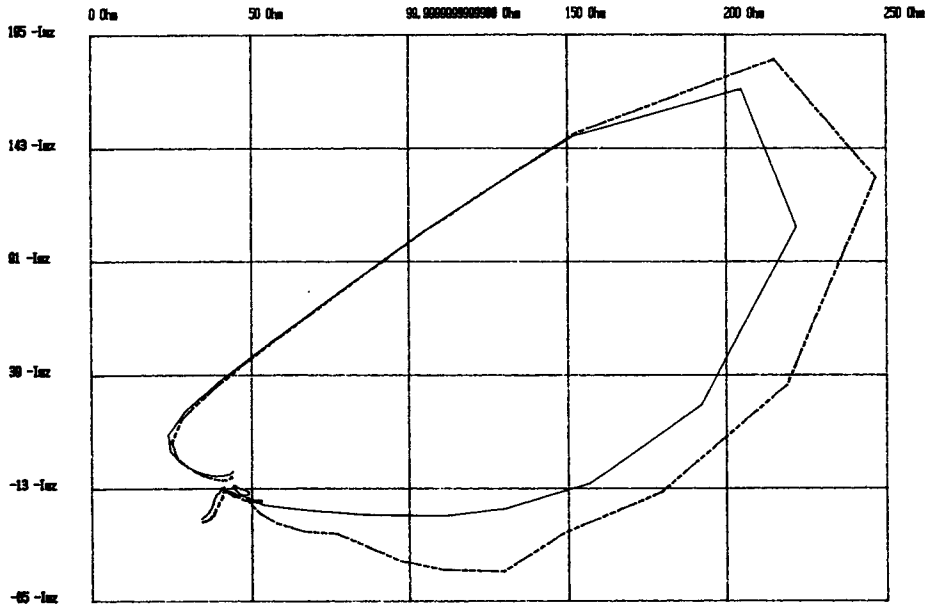

Fig. 6. Variation of the capacitance as a function of impedance modulus of AChE/ChO modified TTF-TCNQ electrode in the presence (dotted line) and absence (solid lines) of 0.3 m*M* acetylcholine.

cate the oxidation of ChO at the electrode surface. The variation of capacitance (imaginary part) as a function of the impedance modulus is given in Fig. 6. These plots are similar to the Nynkvist plots (Fig. 5).

Figure 7 shows the amperometric response of the sensor at the different concentrations of acetylcholine/choline at a potential of 0.225 V vs SCE in 0.5*M* phosphate buffer (pH 7.5). The amperometric response of the sensor on the addition of acetylcholine/choline can be depicted as follows:

$$\text{Acetylcholine} + H_2O \xrightarrow{\text{AChE}} \text{Choline} + \text{Acetic acid} \quad (1)$$

$$\text{Choline}[H_2] + \text{ChO}[\text{FAD}] \longrightarrow \text{Betain} + \text{ChO}[\text{FADH}_2] \quad (2)$$

$$\text{ChO}[\text{FADH}_2] \xrightarrow{\text{TTF-TCNQ electrode}} \text{ChO}[\text{FAD}] + 2H^+ + 2e^- \quad (3)$$

In the above reaction scheme ChO[FAD] and ChO[$FADH_2$] refer to oxidized and reduced forms of the enzyme choline oxidase. The choline formed in step 1 reacts with ChO, resulting in the reduction of the enzyme, which is then oxidized at the surface of the TTF-TCNQ electrode. The response of the sensor on the addition of choline as initial substrate is slightly greater at the same concentration of the acetylcholine.

Kinetic analysis of the variations of current on the substrate concentrations can be done by making Hanes plots ($[S]/j$ vs $[S]$, where $[S]$ and j

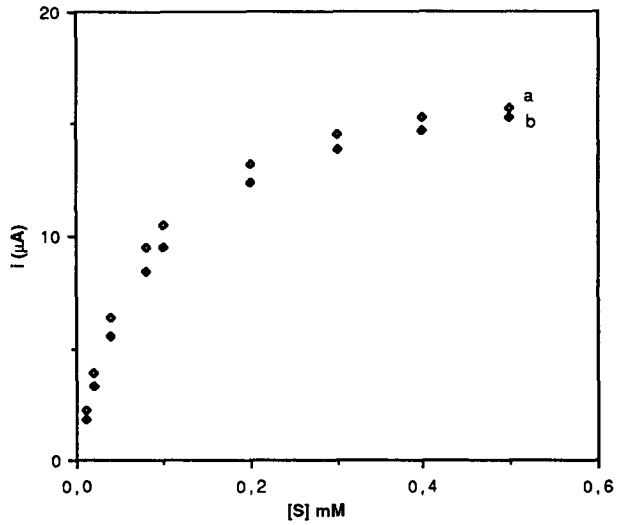

Fig. 7. Response curves for the AChE/ChO modified TTF-TCNQ electrode in 0.5*M* phosphate buffer, pH 7.6, at 30°C: a, choline; b, aceylcholine.

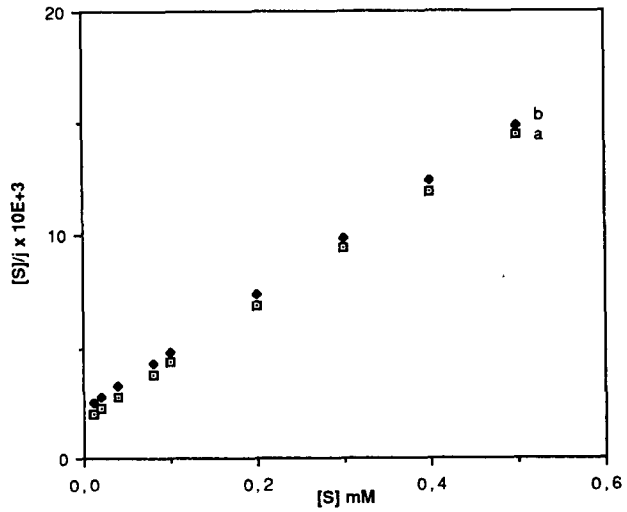

Fig. 8. Hanes plots for the data given in Fig. 7: a, choline; b, acetylcholine.

refer to substrate concentration and fluxes) of the data given in Fig. 7 using the expressions derived by Albery et al. (*1,12,28*). These plots are given in Fig. 8. The intercept $[I]$ of the Hanes plot at zero substrate concentration $[S]$ determines k'_{ME}, the limiting value of the effective electrochemical rate constant for low substrate concentration as described by the expression

$$[1/k'_{ME}] = (I) = ([S]/j)_0 = \{2AF[S]/i)\}_{[S]\to 0} \quad (4)$$

Table 1
Kinetic Results for AChE/ChO Modified TTF-TCNQ Electrode

	Choline	Acetylcholine
k'_{ME}	5.5×10^{-4} (5.7×10^{-4})[a]	4.4×10^{-4} (5.8×10^{-4})[a]
K_{ME}	7.2×10^{-5} (7.9×10^{-5})[a]	9.0×10^{-5} (1.0×10^{-4})[a]

[a]Ref. 2.

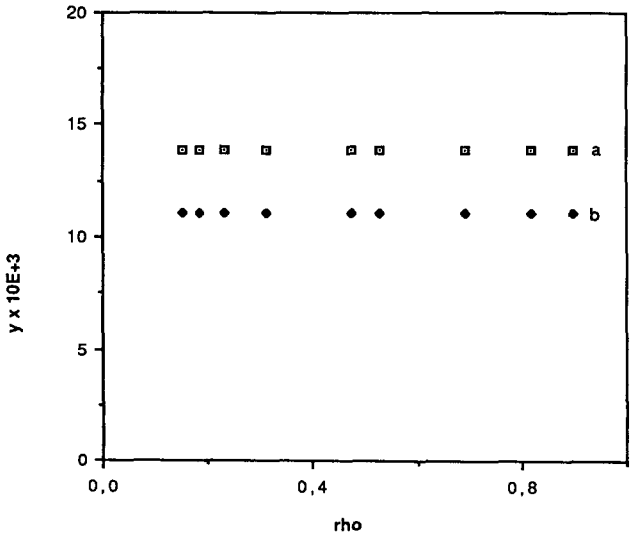

Fig. 9. Plots of the parameters ρ and y for the data given in Fig. 7: a, choline; b, acetylcholine.

where A is the area of the working electrode is the current and F is the Faraday constant. These values are given in Table 1 along with the value obtained by Hale and Wightman (2). Values of k'_{ME} for the detection of choline and acetylcholine are close (Table 1), since the conversion of acetylcholine to choline is very rapid. The next stage of kinetic analysis is the calculation of the value of the effective electrochemical rate constant (K_{ME}) that governed the high substrate concentration. This can be done provided the values of the parameters ρ and y are known; ρ may be estimated using the following relations:

$$\rho = Ij/[S] \tag{5}$$

and

$$y = \{(\rho)^{-1} - 1\}/[S] = (1/K_{ME})\,[1 - \rho k'_{ME}/k'_s] \tag{6}$$

where k'_s refers to the effective electrochemical rate constant for mass transfer kinetics. Plots of y and ρ are given in Fig. 9 for choline and acetylcholine. In each case a horizontal line is obtained, which indicates that k'_s is always much greater than the effective electrochemical rate constant for unsaturated enzyme kinetics (k'_{ME}); hence, unsaturated enzyme kinetics

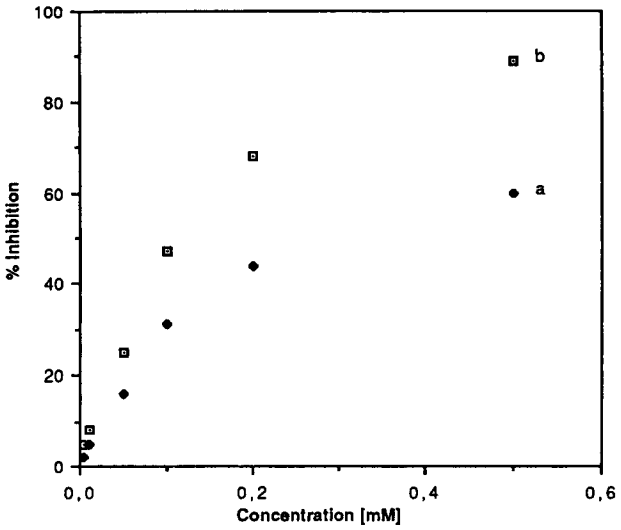

Fig. 10. Determination of (a) fluoride ion and (b) nicotine using AChE/ChO modified TTF-TCNQ electrode in 0.5*M* phosphate buffer, pH 7.5, at 30°C.

is the rate-limiting step. This is in accordance with the earlier observation of Hale and Wightman (2), which is obvious from the model of the present enzyme electrode design, since there is no barrier at the solution/electrode interface. The values of K_{ME} can be obtained from the intercepts of the plots (at $\rho = 0$) given in Fig. 9. These values are recorded in Table 1 along with the values obtained by Hale and Wightman (2), which are very close.

Determination of fluoride ion and nicotine is based on the measurement of percentage of inhibition (I), which is equal to the difference in current obtained by the sensor with and without the inhibitor for the same concentration of the substrate and can be depicted as follows:

$$(I) = \{(I_0 - I_1)/I_0\} \times 100 \quad (7)$$

where I_0 is the current change obtained by the sensor in absence of the inhibitor and I_1 is the current change in presence of the inhibitor at the same concentration of the substrate. These data are given in Fig. 10. The lowest detection limit for these inhibitors is $10^{-6}M$.

REFERENCES

1. Albery, W. J., Bartlett, P. N., Cass, A. E. G., Craston, D. H. and Haggett, B. D. G. (1986), *J. Chem. Soc. Faraday Trans. I* **82,** 1033.
2. Hale, P. D. and Wightman, R. M. (1988), *Mol. Cryst. Liq. Cryst.* **160,** 269.
3. Lindsay, W. S., Kizzort, B. L., Justice, J. B., Salamone, J. D., and Neill, D. B. (1980), *Chem. Biomed. Environ. Instrum.* **10,** 311.

4. Lindsay, W. S., Herdon, J. G., Blakely, R. D., Justice, J. B., and Neill, D. B. (1981), *Brain Res.* **220,** 391.
5. Jaramillo, A., Lopez, S., Justice, J. B., Salamone, J. D., and Neill, D. B. (1983), *Anal. Chim. Acta* **151,** 149.
6. Tran-Minh, C., Pandey, P. C., and Kumaran, S. (1990), *Biosensors Bioelectronics* **5,** 461.
7. Mizutani, F. and Tsuda, K. (1982), *Anal. Chim. Acta* **139,** 359.
8. Karube, I., Hara, K., Satoh, I. and Suzuki, S. (1979), *Anal. Chim. Acta,* **106,** 243.
9. Yao, T. (1983), *Anal. Chim. Acta* **153,** 169.
10. Tsuchida, T. and Yoda, K. (1983), *Clin. Chem.* **29,** 135.
11. Mascini, M. and Moscone, D. (1986), *Anal. Chim. Acta* **179,** 439.
12. Albery, W. J., Bartlett, P. N., and Craston, D. H. (1985), *J. Electroanal. Chem.* **194,** 221, 223.
13. McKenna, K. and Brajter-Toth, A. (1987), *Anal. Chem.* **59,** 954.
14. Freund, M. S. and Brajter-Toth, A. (1989), *Anal. Chem.* **61,** 1048.
15. McKenna, K., Boyette, S. E., and Brajter-Toth, A. (1988), *Anal. Chim. Acta* **206,** 75.
16. Jaeger, C. D. and Bard, A. J. (1979), *J. Am. Chem. Soc.* **101:7,** 1690.
17. Degani, Y. and Heller, A. (1987), *J. Phys. Chem.* **91,** 1285.
18. Kulys, J. J. (1986), *Biosensors* **2,** 3.
19. Kulys, J. J. and Svirmickas, G. J. S. (1980), *Anal. Chim. Acta* **117,** 115.
20. Kulys, J. J. and Samalius, A. S. (1982), *Lietuvos TSR Mokslu Akad. Darbai. B Ser.,* **2(129),** 3.
21. Kulys, J. J. and Cenas, N. K. (1983), *Biochim. Biophys. Acta* **744,** 57.
22. Hendry, S. P. and Turner, A. P. F. (1988), *Horm. Metab. Res.* **20,** 37.
23. Turner, A. P. F., Hendry, S. P., and Hendry, M. F. (1987), Biosensors, Instrumentation and Processing, Online, London, p. 125.
24. Turner, A. P. F., Karube, I., and Wilson, G. S. (1987), *Biosensors: Fundamentals and Applications,* Turner, Karube, and Wilson, eds., Oxford University Press, Oxford, pp. 272.
25. Cenas, N. K. and Kulys, J. J. (1981), *Bioelectrochem. Bioenerg.* **8,** 103.
26. Albery, W. J., Bartlett, P. N. and Cass, A. E. G. (1987), *Philos. Trans. R. Soc. Lond. [Biol.]* **316,** 107.
27. Hill, B. S., Scolari, C. A., and Wilson, G. S. (1988), *J. Electroanal. Chem.* **252,** 125.
28. Albery, W. J. and Knowles, J. R. (1976), *Biochemistry,* **15,** 5631.
29. Trammel, A. M., Simmons, J. E., and Borchardt, R. T. (1984), *Pharm. Res.* **3,** 115.
30. Tran-Minh, C. and Yamani, E. El. (1988), *Junter Electrochemical Detection Techniques in Applied Biosciences* Ellis Horwood, Halsted Press, Chichester, Sec. 1.3, pp. 131.
31. Mayo, S. L., Ellis, W. R., Jr., Crutchley, R. J., and Gray, H. B. (1986), *Science* **233,** 948.